October 13, 2007

Particle deposition and optical response of ITER Motional Stark Effect diagnostic first mirrors

J.N. Brooks, J.P. Allain[1]

Argonne National Laboratory, 9700 S. Cass Ave., Argonne IL 60439, USA
[1] present address Purdue University, W. Lafayette IN, 47907, USA

For submission to Nuclear Fusion

PACS Codes: 52.70.Kz, 52.40.Hf, 52.55.Fa, 52.65.Pp

Contact information:
Jeffrey N. Brooks
brooks@anl.gov
630-252-4830
630-252-3250 fax

Particle deposition and optical response of ITER Motional Stark Effect diagnostic first mirrors

J.N. Brooks, J.P. Allain[1]
Argonne National Laboratory, 9700 S. Cass Ave., Argonne IL 60439, USA

Abstract

Particle deposition/erosion can affect mirrors used in plasma diagnostics and this is a major concern for future fusion reactors. This subject is analyzed for the first and second mirrors of the proposed Motional Stark Effect edge plasma current diagnostic for ITER. Particle fluxes to the diagnostic module aperture are given by edge-plasma/impurity-transport solutions for convective plasma flow for full power fusion conditions. The MC-Mirror code with input of TRIM-SP results is used to compute in-module direct, reflected, and sputtered particle transport. Particles analyzed are D-T and He atoms/ions from the plasma, and Fe, Be, and W from first wall sputtering and/or in-module sputtering. Many of the results are encouraging for optical diagnostic use in ITER, and possibly for post-ITER high duty factor reactors. The LLNL-4B module design analyzed works well in minimizing particle flux to the mirrors, with a factor of ~200-400 reduction in aperture-to-first-mirror flux. Sputtering erosion/degradation of Mo or Rh coated mirrors by incident D, T, and He is negligible. IMD optical effects code analysis shows probably tolerable changes in light reflection and polarization due to mirror beryllium deposition. Tungsten flux to the mirrors is very low. Based on available but limited data, however, there is major concern about the effect of the predicted helium flux on mirror optical properties.

1. Introduction

Numerous ITER diagnostics will employ visible light mirrors in module geometries open to the plasma. An obvious concern is degradation of mirror reflectivity and polarization properties by impinging plasma particles. Impurity particle (Be, W, etc.) deposition can change the mirror surface from the as-fabricated material into another material, while erosion by D, T, He can remove a surface coating and/or affect the surface microstructure. More complex mechanisms could also degrade the first mirror optical properties, including high fluence low-energy He

[1] present address: Purdue University, W. Lafayette IN 47907, USA

implantation leading to bubble formation, surface blistering, and formation of porous deposited layers. A world-wide experimental program to study these issues is underway e.g., [1,2], and some modeling has been done [3 and references therein]. In this paper we analyze particle deposition and mirror response for one typical visible light diagnostic—the edge Motional Stark Effect (MSE) system. We make use of current plasma edge and plasma surface interaction modeling for ITER. Our purpose is to help assess mirror and module material choices, module geometry, and required mirror replacement frequency. Also, by extrapolation we can evaluate the feasibility of having visible light diagnostics on post-ITER high duty-factor fusion devices.

2. MSE Diagnostic

The MSE diagnostic for ITER will measure the plasma current density profile via Doppler-shifted D-alpha emission due to neutral beam/plasma interaction [4]. In particular, the light polarization angle will be measured. An engineering challenge is to design a plasma-facing module to collect the polarized light efficiently while minimizing exposure of the mirrors to plasma particles during the shot. The MSE diagnostic in ITER consists of two systems at separate toroidal and poloidal locations. One system collects light from the edge plasma, the other from the core. An initial edge MSE diagnostic design consisted of two forward mirrors located in the blanket shield module (BSM) of ITER near the outer wall midplane [4]. The new LLNL-4B design [5], shown schematically in Figure 1, is at the same location and also keeps two first mirrors in the BSM for the edge MSE diagnostic, however, having the second mirror with its back to the center of the machine. The new design is the result of a major optimization effort to maximize optical throughput while maintaining polarization, maintaining port-plug neutron shielding, and satisfying several other constraints.

We analyzed both designs. We focus here on results for the LLNL-4B design. This design has a 456 x 60 mm aperture, duct region, and “mirror box” containing primary and secondary mirrors. Distance from the aperture center to the first mirror is 1100 mm. The mirror box is 240 mm in height. The mirrors are approximately circular with diameters 143 and 217 mm respectively. While subject to change, conclusions here should be reasonably applicable to any open-module diagnostic geometry.

3. Particle transport modeling

3.1 MC-Mirror code

The MC-Mirror Monte Carlo code was written to compute in-module particle transport. Code inputs are the particle flux and angular/energy spectrum of particles incident on the diagnostic module aperture (boundary conditions), module geometry, and sputtering/reflection simulation output from the TRIM-SP binary collision surface code.

The LLNL-4B diagnostic geometry is modeled in MC-Mirror with 13 regions including the aperture, top and bottom surfaces, side surfaces, the first and second mirrors, and a misc. zone extending radially. The surfaces are planar with generally irregular shapes.

Particle flux to the mirrors is determined by flux to the aperture, direct particle flow from aperture to the mirrors ("solid angle effect"), in-module particle reflection, in-module sputtering. Processes therefore included in MC-Mirror are: (1) direct transport of aperture-incident particles to all line-of-sight surfaces; (2) reflection of particles from internal surfaces, including multiple reflection, using TRIM-SP code derived energy-dependent particle and energy reflection coefficients; (3) sputtering of internal structure and transport of sputtered material to the mirror; (4) sputtering of aperture-impinging plasma impurities (Be, W, C) from an ion deposition surface to be described, and further internal sputtering; (5) sputtering of the first and second mirrors.

Aperture-impinging particle species analyzed are:

- D, T, He *atoms* from charge exchange (CX) in the edge/scrape-off-layer (SOL) plasma (arising from plasma facing component recycling of the respective ions).
- D, T, He *ions* from plasma transport in the edge plasma extending to the first wall.
- Beryllium ions from sputtering of the reference Be coated first wall, and subsequent core and edge/SOL transport to the first wall/diagnostic-aperture.
- Tungsten ions from sputtering/transport of an alternative W coated first wall.

Internally sputtered particles analyzed are:

- Iron atoms from the reference stainless steel module

- Beryllium or tungsten atoms from sputtering of possible as-installed module coatings and/or coatings resulting from plasma operation.

3.2 Boundary conditions

Aperture-incident boundary conditions for D,T neutrals, and D,T, He, Be, W ions were obtained from studies and model extensions using the US coupled Code Package OMEGA effort [6,7] That work includes computation of the charge exchange D-T flux to the wall/aperture using the DEGAS2 Monte Carlo neutral transport code applied to a UEDGE plasma edge fluid code solution. The computed energy spectrum of D-T neutrals to the wall extends from about 1 eV to 1 keV [6-8].

It is assumed that the diagnostic port is non-perturbing to the edge/SOL plasma, by virtue of its small area compared with the ~800 m^2 first wall area. Thus, particle inputs to the aperture are taken to be the same as to the first wall. We assume no particle-affecting plasma in the module.

Helium transport is not yet fully available from the OMEGA modeling. For He ions, we use a ratio of 5% He/D-T at the first wall, representing the approximate core plasma concentration. For helium charge exchange flux to the first wall we use initial results [8] from DEGAS2 modeling applied to the baseline plasma solution of Ref. [6]. We note that this He CX flux is much higher than that for EIRENE calculations of particle fluxes to an ITER upper port diagnostic location [9], with the difference probably due to the different locations of the modules studied (midplane this study vs. near-top) and plasma conditions (convective edge vs. non-convective). The DEGAS2 He and D-T CX energy spectrums are fairly similar, and both are roughly similar to the EIRENE results.

All results here are for the reference ITER assumption of plasma convective and diffusive edge flow. As discussed in Ref. [6,7] convective ("blob") flow involves a two order of magnitude increase in particle fluxes to the first wall, compared to a plasma with diffusive-only flow. Therefore, this is a much more challenging case for mirror diagnostics than for older non-convective boundary plasma assumptions.

Because of the module geometry no ions can directly hit the mirrors; ions first hit somewhere in the module and then can reflect (D, T, He) or be sputtered (Be, C, W) as neutrals, and these can hit the mirrors. Ion transport to the diagnostic module is a complex process involving edge/SOL plasma transport, plasma density/temperature at the wall, spatially-varying and possibly time-varying toroidal and poloidal magnetic fields, module geometry, finite gyroradius effects, and sheath structure. A rigorous ion impingement computation is beyond the scope of the present effort. Fortunately, a simplified model can be used here which is believed to capture key details of the ion deposition process. In this model:

1) Ions impinge uniformly on the module lower surface on an area extending across the aperture toroidal dimension, and 10 mm radially into the module, as depicted in Figure 1. This is based on the toroidal and poloidal field line structure at the ITER outer midplane and on diffusion considerations. (The 10 mm radial dimension was varied in the code and found be non-critical over a range of 1-30 mm.)

2) Ion impingement energies/angles at this module strike surface are determined by dual-zone (magnetic sheath plus Debye sheath) kinetic sheath structure, due to the oblique incidence/strong magnetic field geometry. For the reference plasma edge temperature at the aperture, $T_e = T_i = 10$ eV, average impingement energies are ~50 eV for D-T ions, ~100 eV for He^{+2}, and average incident angles are about 50° from the surface normal. Beryllium ions impinge at about 45°, while tungsten impinges at more normal incidence.

3.3 TRIM-SP input to MC-Mirror

The sputtering, sticking/reflection of energetic particles with surfaces along the MSE module and first mirrors are simulated using the binary collision approximation (BCA) code TRIM-SP [10] Sputtering and reflection yields and emitted particle energy and angular distributions are calculated for all relevant incident particle/target combinations, at energies 1-1000 eV, and typically at normal and 45° incidence.

It should be noted that use of BCA codes is most appropriate for energies down to about 50 eV, below which collective effects can occur that, ideally, should be computed by molecular

dynamics or similar collective atomistic simulations. Breakdown of BCA codes occurs in particular with the elevation angle distribution of sputtered species, known from experiments to deviate significantly from theory-derived and TRIM-SP-confirmed cosine distribution [11,12]. Accounting for this effect is beyond the scope of this paper and thus the TRIM-SP distributions are used here in all calculations.

3.4 Model limitation

An important model limitation in this study is that we do not treat *mixed-material* effects. For example, for sputtering of beryllium incident on the ion strike points and on the mirror, we use sputter yields for pure Be, not mixed Be/Fe or Be/Mo. This is a reasonable first-order assumption for the light material on heavy material combination, but would need additional assessment for Be as well as other surface materials (C, Fe, Mo, Rh, W, etc.).

4. MC-Mirror code results

The code was run for each incident particle species, for the reference beryllium coated ITER first wall and an alternative tungsten wall, and for the reference stainless steel module and alternative coated module. Each run uses 10^6 incident particle histories (plus module-sputtered histories). A particle hitting a surface can reflect and/or sputter—as determined by TRIM-SP output. A reflected particle has velocity determined by TRIM-SP distributions (with the numerical simplification of generally choosing the incident angle closest to either 0 or 45° incidence from the surface-normal). A particle history terminates upon non-reflecting at a module surface (sticking or desorbing at thermal energy), or upon leaving the computational region.

Table 1 shows MC-Mirror results for the reference stainless steel module. Key trends are:

For charge exchange D-T incident on the aperture, the D-T flux to the first mirror is reduced by a factor of ~200. The higher energy (> 10 eV) portion of this flux is about 25% of the total. Flux to the second mirror is due entirely to internal reflection, and is reduced by three orders of magnitude from the aperture value. For D-T ions entering the aperture, the flux reduction ratio is ~400 for the first mirror, and ~3000 for the second.

Therefore, the module design is a good one from the standpoint of minimizing D-T flux to the mirrors.

Helium flux to the mirrors is likewise highly reduced from aperture values. The mirror flux from He ions to the boundary is ~30 times higher than due to helium charge exchange. However, the charge exchange energy spectrum extends to much higher energies.

The net flux of beryllium (deposition minus sputtering erosion) to both mirrors is about equal to the gross flux shown because erosion at the mirror is much less than deposition. This is due primarily to differences in sputter yields for D-T neutrals hitting the mirror at about normal incidence, as opposed to oblique incidence at the Be ion strike surface and other module surfaces.

Tungsten flux to both mirrors is very low. This is due to several effects: Sputtering of an ITER tungsten wall is very low to begin with, compared to beryllium. Of the tungsten impinging on the module strike surface, only about 10% is sputtered, so this is a rate-limiting step. Of the tungsten sputtered, only a low percentage hits the mirrors (as with beryllium).

Table 2 shows selected performance differences between the reference bare stainless steel module structure and alternative Be and W coatings. The D-T flux to the first mirror from CX varies by about a factor of two over the material choices analyzed. This is due to differences in particle reflection, being lower for Be and higher for W. A similar trend (not shown) is seen for aperture-impinging ions. There are also differences in energy spectrum, with higher energies resulting from higher energy reflection coefficients of the higher-Z materials. Based on the computed fluxes of module-sputtered material to the aperture/edge-plasma, and considering the small aperture area, there is little concern about core plasma contamination for all three module materials. Also, net growth rates (not shown) due to internal module sputtering is zero for the first mirror, for all materials, and for the second mirror is very low for Be and negligible for ITER for W or Fe coatings. Based on these results there is little motivation for coating the module prior to installation. Also, if the module became internally coated with Be or W during

the course of ITER operation, there would seem to be no major implications for the mirror performance.

5. Effects on mirrors

5.1 Lifetime of first mirror due to D, T, He sputtering

Here we assess lifetimes of candidate molybdenum and rhodium coated first-mirrors under exposure to D, T, and He. (We ignore for this purpose erosion/deposition from impurity particles). Figure 2 shows the TRIM-SP computed sputtering yield curves of Mo and Rh for the typical case of normal incidence at the first mirror. The MC-Mirror code, with inputs of these energy-dependent yields, was used to compute the total erosion rates for the higher sputtering case of a Rh first mirror, for all D, T, and He fluxes of Table 1.

This Rh first mirror erosion rate is 2.7 $x10^{-5}$ nm/s. This is mostly due to D-T CX flux, with a small effect of He CX, and no effect of D-T or He boundary ions since energies for these ions are all below the Rh sputtering threshold. For a 400 sec ITER shot, we have a mirror erosion rate of .011 nm/ shot. This leads to a coating loss of ~0.05 μm Rh in a 5-yr operation cycle with 1000 ITER shots/yr. Since the coating thickness of most mirrors contemplated ranges between 1-10 μm, and optical properties should not be degraded due merely to erosion (for at least single crystal mirrors, e.g., see Ref. [1]), we conclude that sputtering degradation of the diagnostic first mirrors is not a significant problem.

5.2 Hydrogen implantation effect on mirror optical properties

Implantation of the mirrors with hydrogen isotopes should not have a significant negative effect on the optical properties of the mirror based on H_2 irradiation effects studied by Yoshida et al. on candidate first mirror materials (W, Rh and Mo) [13]. In this case, mirrors were exposed to energies 1-10 keV and fluences above 3 x 10^{22} m^{-2} with no observable damage to the surface and no reflectivity degradation. No data exists for fluences greater than 10^{23} m^{-2}, therefore further experimental studies must assess this issue. Unlike the Be case, computational analysis with IMD, to be described, is not possible since optical constants for a hydrogenated metal do not exist.

5.3 Optical response of mirrors with Be deposition

As shown in Table 1 there is a predicted transfer of wall sputtered beryllium to the first and second mirrors of the diagnostic module. Using Table 1 results, and nominal ITER reference of 1000 shots at 400 sec/shot for one year operation in ITER, there would be ~200 nm of Be in one year deposited on the first mirror. We used the IMD code [14] to determine the effect of such deposited Be on mirror reflectivity for the relevant spectral range of the MSE diagnostic (~200-900 nm). The analysis uses the optical geometry in IMD used by Yoshida et al. [15], with a 7.5° incident half-angle for comparison. We studied two primary materials: Mo and Rh. Both use refractive index and extinction coefficient data from Palik et al. [16] for crystalline Mo and Rh structures, and are applied as well as for Be deposits. In these studies we assume no intermixing (optical properties for pure Be, Rh, and Mo are used). It is also assumed that Be deposits layer by layer (e.g. one monolayer at a time). This is a reasonable assumption since the deposition energy of Be atoms lies in the hyperthermal regime (E < 50 eV). However, laboratory data suggests that Be deposits on Mo mirrors may not consist of conformal layers but rather a complex morphological structure with detrimental implications to reflectivity in the visible spectral range due primarily to porous film morphology [17]. Nevertheless the IMD simulations can at least give some indication of response to Be layer deposition on first mirrors used in the MSE diagnostic system.

The specular reflectivity as a function of wavelength is shown in Figure 3 for pure Mo and Rh, and for various Be overlayers. The IMD result for pure Mo is consistent with measured data by Yoshida et al., therefore providing an appropriate benchmark. For wavelengths of 200-900 nm and incident angle of 7.5°, the specular reflectivity does not change more than 5% for Be depositions ranging from 10-100 nm, again assuming that morphological changes are absent. The absolute reflectivity reaches about 0.55-0.60 for a spectral range between 350-900 nm. In the case of Rh, the specular reflectivity at 600 nm, for example, decreases from 0.76 to 0.60 or a significant 21% drop. The results for 100 nm Be are essentially identical to pure Be (due to the e-folding length of the evanescent wave in the material surface). Therefore, after about a half year full-power operation in ITER, the mirrors would essentially function as Be mirrors.

Another potential effect of Be mirror deposition is on variation of reflected light polarization. IMD simulations were run for the two mirror materials and Be film thicknesses at a single wavelength of 600 nm while varying the incident light angle between 0-90°, and selected results are shown in Figure 4. The total reflectance is computed with respective s and p polarization vectors. The first case has the incident light with an incident polarization factor, f = 0, (unpolarized light or polarized light in all directions). The next two cases use an incident polarization factor f = 1.0 and f = 0.33, however for clarity we show the f = 1.0 case for Mo and Rh in Figure 4. The polarization factor is defined as $f = \frac{I^s - I^p}{I^s + I^p}$ and the linear polarization fraction is the ratio of R_p/R_s from the simulations for deposition of 100 nm of Be. Results show that only in the case for a Rh mirror that is eventually covered with Be, the polarization linear fraction decreases by > 50% for incident angles between 75-85° incidence (with respect to the mirror surface).

5.4 Effects of He exposure on first mirror

There is no data available on the combined effects of simultaneous D, T, He impingement on mirror performance, let alone with possible simultaneous Be, etc. buildup. There is limited data on elevated temperature performance, and on low energy (< 100 eV) He implantation. In this section, therefore, we restrict the analysis to roughly assessing the MC-Mirror results in light of the important but limited data that does exist.

Studies by Yoshida et al. [13,15,18] of He^+ irradiation of Mo polycrystalline mirrors for energies between 1-8-keV show an incident He fluence threshold between 1-3 x 10^{22} m^{-2} for surface damage resulting in specular reflectivity losses between 20-40% at a spectral range between 200-900 nm from RT up to 873K. At these fluences, formation of blisters and large scale roughening with fine bubble formation near the surface lead to this moderate decrease in reflectivity. At higher fluences, > 3-5 x 10^{22} m^{-2}, a porous structure near the surface was generated due to the formation of highly dense He bubbles at nanometer scale, also enhancing roughness to levels near 100 nm rms and decreasing the reflectivity by factors between 2-5.

For fluences below 10^{22} m^{-2}, the formation of fine bubbles around the He projected range was hypothesized by the Yoshida group and a weak influence of the mirror surface roughness on the reflectivity was measured. (However, recent data [15] shows that even fluences between 1-3 x 10^{21} m^{-2} can induce reflectivity losses.)

Temperature effects on He bubble formation in candidate mirror materials have also been studied by Yoshida et al. [18]. Temperature increase of candidate first mirror materials generates thermally excited defects, and coupled to He irradiation leads to stable bubble formation at fluences above 10^{21} m^{-2}. There is an isolated case with TEM data showing He bubble formation in the sub-threshold energy regime (~250 eV) at irradiation fluences of 10^{21} m^{-2} and 873K for a W sample. For certain heat treatments (e.g., laser ablation) He bubbles can be annihilated by He bubble migration to the mirror surface and bubble recombination. Ablation can be enhanced by the new microstructure formed during He implantation and migration, in particular at larger fluences (> 10^{23} m^{-2}) where additional small bubbles and holes can be formed at the mirror surface lowering the surface thermal conduction. Other work using the DiMES probe in DIII-D has alluded to the self-healing of Mo mirrors, recovering specular reflectivity from an increase in temperature of the mirror to levels between 90-200 °C [1].

What could these results mean for ITER? Due to model uncertainties we consider separately the effects of the two sources of He to the mirror, viz. charge exchange and ion transport. With nominal ITER shots of 400 seconds and 1000 ITER shots/yr, the one-year fluence of He to the first mirror due to He^{+2} ion impingement on the strike surface is ~2 x 10^{22} m^{-2} at an average energy of < 30 eV, using MC Mirror code results. As mentioned, this energy is much lower than for existing data; also the first wall/diagnostic will be operated at elevated temperature (~250°C). Assuming, however, that the Yoshida et al. He fluence threshold of ~10^{22} m^{-2} nevertheless applied, this would give on the order of 1 year operation before significant effect (reduced reflectivity) occurred. However, it is reasonably possible that operation would be extended due to the much lower average impingement energy compared with the > 1 KeV data. Alternatively, multi-particle synergistic effects and material microstructural effects could make things worse. It is obvious that further computational work and laboratory experiments are needed in this area.

The He CX neutral mirror flux, at ~1-1000 eV energy spectrum, reaches a fluence of 2 x 10^{21} m^{-2} for the same ITER shot history. All other things being equal, this would imply a 5 X longer operating window, compared to the effects of He ions.

From Table 1 we also note that the He flux to the second mirror is about an order of magnitude lower than at the first mirror, thus presumably implying a 10 fold greater lifetime with respect to helium effects.

5.5 Post-ITER Implications for MSE diagnostic

We assume here direct extrapolation of the present ITER results to a DEMO or commercial fusion reactor, with scaling due to duty-factor only. With respect to erosion induced by D-T bombardment, the erosion rate of order 1 μm/year would permit multi-year operation between mirror coating replacements. Therefore we find D-T induced erosion in a commercial fusion reactor to be negligible.

With respect to Be deposition, the use of a Be first wall in a commercial reactor is prohibitive due to erosion alone. Hence, W would be a likely first wall material due to much lower sputtering erosion [6]. From MC-Mirror analysis there is no net buildup of tungsten on the first or second mirror due to first wall sputtering, the code predicting that tungsten would be sputtered as fast as deposited. There would likewise be no buildup of iron, from module sputtering, on the first mirror. For the second mirror, however, the code predicts an iron buildup rate of 7.9 x10^{-15} m/s. For 75% duty factor this would give about a ~200 nm iron layer on top of the second mirror surface per year. Alternatively, a tungsten coated module would yield a ~10 nm/year second-mirror growth. These scenarios appear tolerable.

For incident He flux to a mirror operating with high duty factor, a He fluence of $> 10^{22}$ m^{-2} would be reached in several days. If such fluence did, in fact, result in the formation of nanoscale bubbles and blister generation on mirror surfaces leading to high specular reflectivity loss, than the MSE diagnostic would be seriously impaired almost immediately. Therefore, the issue is whether such effects occur and/or can be ameliorated, for the realistic case of multi-particle simultaneous bombardment, at elevated temperatures, with mixed-material and other

differences. For the case of higher first wall/diagnostic module temperatures in a commercial fusion reactor, the resulting morphology on a candidate mirror material needs further study, since a balance between formation of thermally-activated defects supporting bubble formation and migration of bubbles to the surface with subsequent annihilation is established and largely depends on the incident irradiation and mirror material. Possible solutions also include use of alternative mirror materials.

6. Model variations

We briefly assessed the sensitivity of the results to several model variations as follows:

6.1 Module baffles

The idea of baffling is to reduce internally reflected and sputtered particle fluxes to the mirrors while not affecting photons. We modeled the addition of several small side/top/bottom baffle plates to relevant surfaces in the MC-Mirror module geometry, and also modeled a variation in the aperture design to provide for a more realistic neutron heat-removal design [19]. The results show only a small (~15%) effect in reducing mirror particle fluxes. The reason is that most aperture-incident particles and internally reflected and sputtered particles travel along the same paths as the photons, and hence are not baffled.

6.2 Plasma boundary temperature

The reference plasma wall/boundary temperature of 10 eV is uncertain. This parameter affects incident ion energies and reflection and sputtering coefficients. We ran the MC-Mirror code for boundary temperature cases of 5 eV and 20 eV, corresponding to incident D-T ion energies of 25 and 100 eV respectively (with sheath acceleration). At the lower temperature the first-mirror beryllium flux is reduced by a factor of 2.5 due to a reduction in D-T ion sputtering at the strike surface. There is little difference from reference results at the higher temperature—all Be is sputtered from the strike surface (both from ions and CX atoms). Another effect is a small increase (~15%) in D-T flux to the first mirror at the lower temperature, due to higher reflection, and a corresponding small flux decrease at the higher temperature. A potentially more important effect is an increase in helium atom energies to the mirror at higher Te. The effect on mirror performance, if any, would need assessment, as discussed above generally for helium effects.

6.3 Carbon

A flux of energetic carbon to the diagnostic module could occur due to carbon release at the divertor target, such as from plasma ELM heating, and subsequent transport through the core/edge plasma. In our model the mechanism for such carbon to reach the mirrors is the same as for wall sputtered beryllium. Carbon ions would first impinge on the aperture strike surface, then be sputtered and/or reflected from that surface, and then hit the mirror(s) directly or via subsequent sputtering/reflection. (For the reference plasma conditions used here there would be no sputtering of a pure-carbon deposited strike surface by incident D-T ions due to below-threshold energy; all sputtering would be due to CX atoms.) For a carbon ion flux at the aperture of 1% of the D-T ion flux, the carbon flux to the first mirror is found to be about an order of magnitude less than the beryllium flux. However, a mixed-material analysis including consideration of mixed Be/C or C/Fe surface formation/erosion, would be required for a rigorous analysis of carbon transport. Similar considerations apply to other potential plasma impurities.

7. Malaquias MSE Module Design Analysis

We compared particle transport/deposition in the new LLNL-4B MSE design to the initial diagnostic design (MP) by Malaquias et al. [4]. There are three main differences: 1) deposition of Be ions from first wall sputtering and transport to the first mirror is 13 times lower for the LLNL-4B design compared to the MP design; 2) He ion derived flux to the first mirror is reduced by a factor of 4. This is important since otherwise the He ion fluence for 1 year ITER operation would be about 10^{23} m^{-2} where there is possibly an order of magnitude reflectivity loss of the mirror, as discussed earlier; 3) D-T induced erosion is reduced by a factor of about 5 in the new design, although, as mentioned, this is not as serious an issue due to the low sputter rate from Rh and Mo mirrors bombarded by energetic D-T.

8. Conclusions

This work analyzes the transport of plasma fuel and helium particles and external and internally sputtered particles to the first mirrors of the proposed ITER edge plasma MSE diagnostic system. The transport results were used to assess effects on mirror performance, given an existing but sparse data base.

The LLNL-4B module design is efficient in minimizing particle flux to the first and second mirrors, with 2-3 order of magnitude reduction from aperture flux to first and second mirror flux. This is about 10 X better than the initial, less-optimized design. D-T atom flux to the mirrors, with energy spectrum ~1-1000 eV, is mostly (~80%) due to plasma charge exchange. For the energy range > 10 eV the contributions from CX and aperture impinging ions are about equal. The D-T ion flux to the module aperture is significant due to edge plasma convective flow. In general, the MSE diagnostic mirrors should work well in terms D-T impingement, with low erosion and low effect of implantation /surface-content predicted for Mo and Rh mirrors

Beryllium atoms from first wall sputtering impinge on the mirrors at a flux of about 1/100 of the D-T flux. This leads to ~200 nm growth of Be on the MSE first mirror in one year of operation in ITER. This does not have a major effect on specular reflectivity in the 200-900 nm spectral range. However, the analysis does not treat possible changing morphology evolution of the deposited Be thin layer (i.e., porous Be structure can lead to reduction in reflectivity. Further analysis and experiments are needed to correlate Be thin-coating morphology to photon reflectivity loss.

Tungsten flux, from a tungsten coated first wall, is about 2000 times lower than Be. Thus, tungsten is preferable to beryllium from the standpoint of optical diagnostic use.

For ITER, there is no apparent compelling reason to coat the diagnostic module surfaces prior to installation (but that could change for a high duty factor device). A bare stainless steel module has performance substantially similar (factor of 2) to a low-Z (Be) or high-Z (W) coating. Internal sputtering of module material should not significantly contaminate the core plasma. Use of baffles to reduce mirror particle deposition is not effective.

The most serious concern appears to be the effect of non-thermal helium flux on the mirrors. The mirror He atom flux due to He ion edge transport is about ten times greater than due to charge exchange, however with significant energy differences. Both sources of He can lead to surface damage and order of magnitude lower reflectivity (for fluences well above 10^{22} m^{-2}) of Mo and Rh mirrors at room temperature, based on experimental data by Yoshida et al.. ITER

MSE diagnostic use, however, may be acceptable, with perhaps multi-year operation possible before needed mirror replacement. Further computational work and laboratory experiments are critically needed in this area.

For commercial-grade fusion reactors the most serious challenge to the use of an MSE diagnostic system likewise appears to be the helium damage issue.

The transport part of this analysis has two general uncertainties. First, are the edge/sol plasma properties, including ion transport near and to the module. In this context, the model for ion impingement on the module is more speculative than the charge exchange model. This particularly affects the He and Be mirror flux computations. The key model uncertainty for in-module calculations is the effects of mixed-materials on sputtering and reflection.

There are additional mechanisms not covered in this analysis. This includes the cracking of background hydrocarbons on mirror surfaces induced by UV light. In this case the intensity of light must be high enough to induced contamination on the mirror surface. This may be important for regions around the ITER diagnostic ducts and should be included in future work.

Acknowledgement

This work was supported by the U.S. Department of Energy, Office of Fusion Energy.

References

[1] A. Litnovsky et al., J. Nucl. Mater. 363-365(2007)1395.

[2] A.J.H. Donne, Nucl. Fusion 47 (2007)833.

[3] V. Voitsenya, et al., Rev. Sci. Instrum. 72,1(2001)475.

[4] A. Malaquias, et al., Rev. Sci. Instrum. 73,3393(2004).

[5] S. Allen et al., *Evaluation of ITER MSE Viewing Optics,* LLNL Report 2007.

[6] J.N. Brooks, J.P. Allain, T.D. Rognlien, Physics of Plasmas 13(2006)122502.

[7] T.D. Rognlien, R.H. Bulmer, M.E. Rensick, J.N. Brooks, J. Nucl. Mater. 363-365(2007)658.

[8] M. Rensick, LLNL, Pers. Comm. 2007.

[9] V. Kotov, IPP Julich, Pers. Comm. 2007.

[10] W. Eckstein, *Computer Simulation of Ion-Solid Interactions,* Springer-Verlag, Berlin 1981.

[11] E. Oyarzabal, J. H. Yu, R. P. Doerner, and G. R. Tynan and K. Schmid, J. Appl. Phys, 100 (2006)063301.

[12] D. Nishijima et al., Proc. 32nd EPS Conference on Plasma Phys., ECA Vol. 29C(2005)P4.010.

[13] N. Yoshida, et al., "Effects of He Bombardment on Surface Morphology and Optical Reflectivity", 9th Meeting of the ITPA Topical Group on Diagnostics, Daejeon, Korea, 10-13 October 2005.

[14] D.L. Windt, Computers in Physics, 12(4)(1998)360.

[15] N. Yoshida et al., "Reduction and Recovery of Optical Reflectivity of Mo Mirror Irradiated by Low Energy Helium Ions," 12th Meeting of the ITPA Topical Group on Diagnostics, Princeton, New Jersey, USA, 26-30 March, 2007.

[16] E.D. Palik, in Handbook of Optical Constants of Solids, 1985, eds. Lynch and Hunter, Academic Press.

[17] G. De Temmerman et al., Proc. 32nd EPS Conference on Plasma Phys., ECA Vol. 29C (2005)P1.076.

[18] N. Yoshida, H. Iwakiri, K. Tokunaga and T. Baba, J. Nucl. Mater. 337-339(2005)946.

[19] D. Johnson, PPPL, Pers. Comm. 2007.

Table 1. Particle transport to first and second mirrors of ITER MSE LLNL-4B edge plasma diagnostic, for particles impinging on the outer midplane first wall/diagnostic aperture. For reference stainless steel diagnostic module. All results for convective plasma edge regime.

.

Particle type to aperture	**Particle flux to aperture** $m^{-2}\ s^{-1}$	**Resulting atom flux to first mirror*** $m^{-2}\ s^{-1}$	**Resulting atom flux to second mirror*** $m^{-2}\ s^{-1}$
D-T charge exchange atoms (full energy spectrum)	7.21×10^{20}	3.96×10^{18}	6.29×10^{17}
D-T charge exchange atoms (> 10 eV spectrum)	2.56×10^{20}	1.29×10^{18}	1.62×10^{17}
D-T ions (from plasma edge)	3.59×10^{20}	9.10×10^{17}	1.21×10^{17}
He charge exchange atoms (full energy spectrum)	6.50×10^{17}	4.26×10^{15}	6.55×10^{14}
He ions (from plasma edge)	1.80×10^{19}	4.55×10^{16}	6.05×10^{15}
Be ions (from first wall sputtering of reference Be wall)	1.47×10^{19}	5.81×10^{16}	7.71×10^{15}
W ions (from first wall sputtering of alternative W wall)	8.71×10^{16}	2.68×10^{13}	~0

* For D-T, He atoms: by direct flow from aperture and in-module reflected flow. For D-T, He ions: by reflected flow from ion strike surface and further in-module reflection. For Be and W ions: by sputtering at ion strike surface and further in-module sputtering.

Table 2. Particle transport as a function of module material.

Module Material	**D-T atom flux to mirror [a]: first mirror (second mirror)** $m^{-2}\ s^{-1}$	**Module material flux to mirror [b]: first mirror (second mirror)** $m^{-2}\ s^{-1}$	**Module material flux to aperture (output to edge plasma)[b]** $m^{-2}s^{-1}$
Iron (stainless steel structure)	1.29×10^{18} (1.80×10^{17})	4.41×10^{15} (8.24×10^{14})	1.12×10^{18}
Beryllium (coating)	9.74×10^{17} (2.95×10^{16})	1.20×10^{16} (4.76×10^{15})	1.08×10^{19}
Tungsten (coating)	1.65×10^{18} (3.10×10^{17})	8.99×10^{13} (2.66×10^{13})	3.05×10^{16}

a) due to D-T from charge exchange, > 10 eV spectrum; flux to aperture = $2.56 \times 10^{20}\ m^{-2}\ s^{-1}$
b) due to internal module sputtering by both aperture-incident D-T atoms and ions.

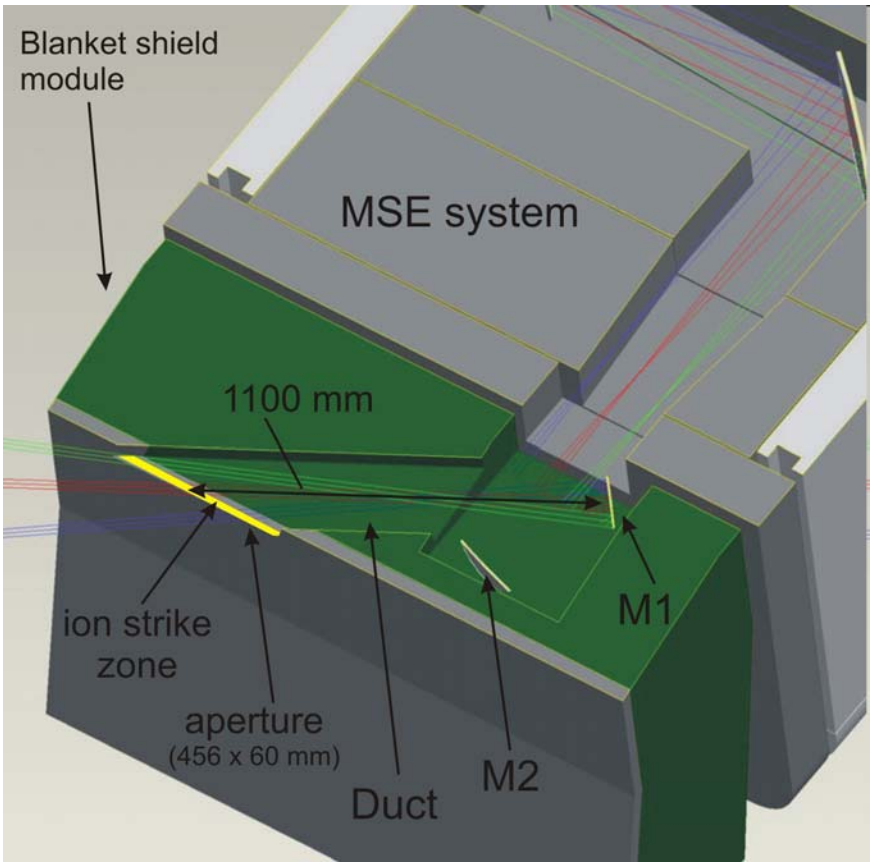

Figure 1. LLNL-4B MSE diagnostic geometry at ITER outer midplane first wall location. Optical path shown through blanket shield module (BSM) duct with first 2 mirrors (M1, M2). Plasma ion strike-point deposition zone shown. (Adapted from ref. 5).

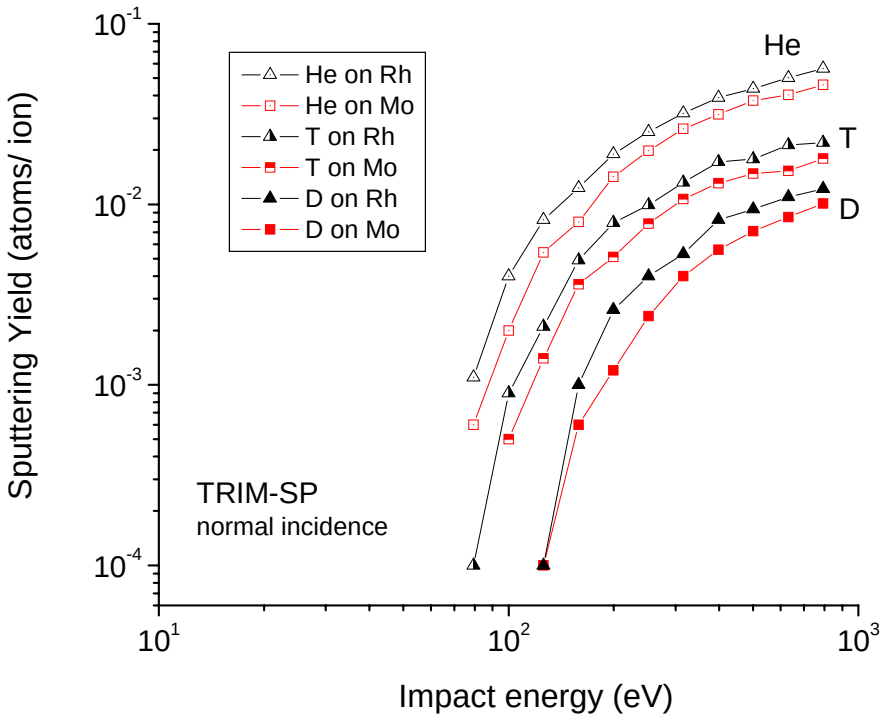

Figure 2. Sputter yield of candidate mirror materials as a function of impact energy by D, T and He at normal incidence.

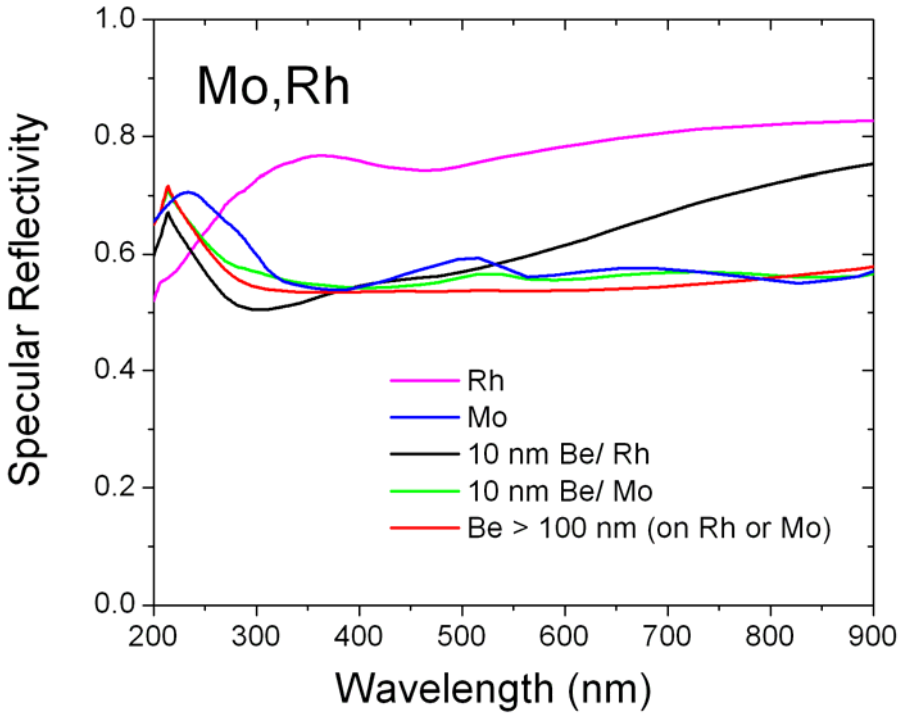

Figure 3. Reflectivity of Mo and Rh mirrors in the spectral region between 200-900 nm for various Be deposition thicknesses. IMD code analysis.

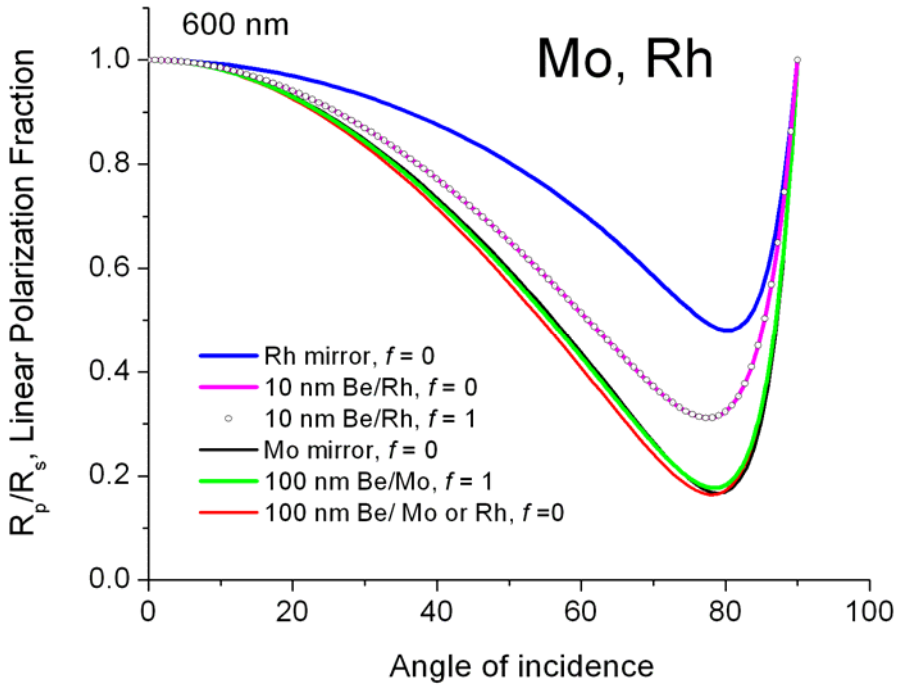

Figure 4. IMD simulation results for f = 0.0 and 1.0 with 600-nm light on Mo and Rh for 0 and 100 nm Be deposition thickness.